Journal of Heredity, 2022, **113**, 398–413
https://doi.org/10.1093/jhered/esac018
Advance access publication 6 April 2022
Original Article

Original Article

CRISPR Knockouts of *pmela* and *pmelb* Engineered a Golden Tilapia by Regulating Relative Pigment Cell Abundance

Chenxu Wang, Jia Xu, Thomas D. Kocher, Minghui Li, and Deshou Wang

From the Key Laboratory of Freshwater Fish Reproduction and Development (Ministry of Education), Key Laboratory of Aquatic Science of Chongqing, School of Life Sciences, Southwest University, Chongqing 400715, China (C. Wang, Xu, Li, and D. Wang) and Department of Biology, University of Maryland, College Park, MD 20742, USA (Kocher).

Address correpondence to De-Shou Wang and Minghui Li at the address above, or e-mail: wdeshou@swu.edu.cn and limh@163.com

Corresponding Editor: Bridgett vonHoldt

Abstract

Premelanosome protein (*pmel*) is a key gene for melanogenesis. Mutations in this gene are responsible for white plumage in chicken, but its role in pigmentation of fish remains to be demonstrated. In this study, we found that most fishes have 2 *pmel* genes arising from the teleost-specific whole-genome duplication. Both *pmela* and *pmelb* were expressed at high levels in the eyes and skin of Nile tilapia. We mutated both genes in tilapia using CRISPR/Cas9. Homozygous mutation of *pmela* resulted in yellowish body color with weak vertical bars and a hypopigmented retinal pigment epithelium (RPE) due to significantly reduced number and size of melanophores. In contrast, we observed an increased number and size of xanthophores in mutants compared to wild-type fish. Homozygous mutation of *pmelb* resulted in a similar, but milder phenotype than *pmela*$^{-/-}$ mutants. Double mutation of *pmela* and *pmelb* resulted in loss of additional melanophores compared to the *pmela*$^{-/-}$ mutants, and also an increase in the number and size of xanthophores, producing a golden body color. The RPE pigmentation of *pmela*$^{-/-}$;*pmelb*$^{-/-}$ was similar to *pmela*$^{-/-}$ mutants, with much less pigmentation than *pmelb*$^{-/-}$ mutants and wild-type fish. Taken together, our results indicate that, although both *pmel* genes are important for the formation of body color in tilapia, *pmela* plays a more important role than *pmelb*. To our knowledge, this is the first report on mutation of *pmelb* or both *pmela*;*pmelb* in fish. Studies on these mutants suggest new strategies for breeding golden tilapia, and also provide a new model for studies of *pmel* function in vertebrates.

Graphical Abstract

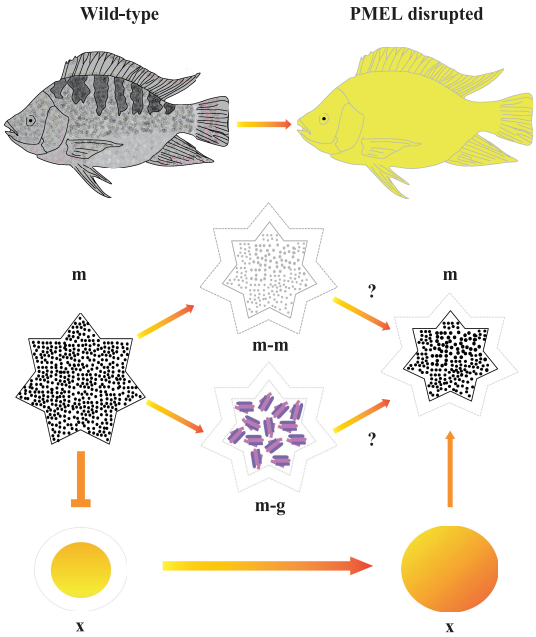

Received January 27, 2022; Accepted April 1, 2022

Subject area: Animal pigmentation genetics in ecology, evolution, and domestication
Key words: *pmel* duplicates, melanin, melanophores, xanthophores, body color, RPE pigmentation, golden tilapia, CRISPR/Cas9 gene editing

Body color and pattern is of great significance for environmental adaptation and survival in vertebrates (Hoekstra 2006; Hubbard et al. 2010; Hofreiter and Schöneberg 2010). Some reports have also pointed out that teleost adaptation to extreme environments, such as cavefish and some deep-sea fish, is often associated with the degeneration of eyes and reduction in skin pigmentation. These changes are usually due to mutation or loss of pigment-related genes (Klaassen et al. 2018; Bilandžija et al. 2018; Wang et al. 2019; Zhao et al. 2019). For instance, the *mc1r* (Stahl and Gross 2015; Espinasa et al. 2018) and *oca2* (Gross and Wilkens 2013; Bilandžija et al. 2013; Bilandžija et al. 2018; Klaassen et al. 2018) have been reported to be the major locus for pigment loss in some cavefish. In recent studies, *pmelb* has also been suggested to be closely linked with melanin loss in some cavefish and deep-sea fish, as the amino acid sequence of this gene was significantly different among species (Bian et al. 2021). These results indicate that *pmel* might be of great significance for teleost adaptation and evolution.

Melanophores are the most widely distributed and most important pigment cells in protecting animals from UV irradiation and oxidative stress (Yamaguchi and Hearing 2009; Ito and Wakamatsu 2011). Many genes are important for melanin biosynthesis, including *pmel*, are regulated by the transcription factor *mitf* (Braasch et al. 2009; Hou and Pavan 2008; Wang et al. 2014). Studies in a variety of vertebrates indicate that *pmel* is fundamental for melanin maturation and deposition (Kerje et al. 2004; Hellström et al. 2011; Ishishita et al. 2018; Lahola-Chomiak et al. 2019) and involved in many pigment cell diseases (hypo- or hyperpigmentation skin diseases like albinism, vitiligo, and melanoma). In studies of humans, *pmel* (also known as *silver*/*gp100*) is a key factor for vitiligo (Yuan et al. 2019). Mutations of this gene also result in abnormal pigmentation of the retinal pigment epithelium (RPE) and known as ocular pigment dispersion and pigmentary glaucoma (Lahola-Chomiak et al. 2019). Studies in mice indicate that variation in *pmel* affects the shape of melanosomes, with subtle effects on visible coat color (Kwon et al. 1994; Hellström et al. 2011). Variation in *pmel* is also associated with dominant white plumage in farmed chicken (Kerje et al. 2004). Most teleosts have 2 *pmel* genes arising from the teleost-specific genome duplication. In the cichlid fish *Haplochromis latifasciatus*, *pmela* shows significantly higher expression in black vertical bars than in light pigmented interbars, which suggests that *pmela* might be involved in bar formation (Liang et al. 2020). Knockout of *pmela* in larvae zebrafish (*Danio rerio*) causes defects in eye development and pigmentation of the RPE and the skin (Lahola-Chomiak et al. 2019). To date, no loss of function studies have been conducted in teleosts of *pmelb* single mutation and *pmela;pmelb* double mutation.

There are 4 phases in melanosome development. First, phase I melanosomes develop from endosomal membranes. The formation of PMEL fibrils gradually converts phase I to phase II melanosomes. Only after the fibrillar structures are formed does melanin begin to be deposited to create phase III melanosomes. The mature phase IV melanosome has a high concentration of melanin. Melanin biosynthesis is directly controlled by genetic factors whose expression is regulated by the melanocyte-inducing transcription factor *mitf*, including the tyrosinase family genes, the iron channel *oca* family genes, the *bloc* family genes, the *slc* family genes, the *hps* family genes and the *pmel* genes. In addition, cell intrinsic environmental factors like the cell membrane electrification, pH levels and the concentration of metal ions (Na^+, K^+, Ca^{2+}, Mg^{2+}, etc.), also have critical effects on melanin synthesis (Yamaguchi and Hearing 2009; Ito and Wakamatsu 2011). PMEL has been acknowledged to play the similar role with tyrosinase and HPS family members, by affecting the transition of melanosomes from phase I to phase II (Ishishita et al. 2018). However, even though some studies have confirmed the role of *pmel* in tetrapod body color formation, mutations in this gene have been found to not always have the same effects on melanin biosynthesis and melanosome shape in different vertebrates (Kerje et al. 2004; Hellström et al. 2011).

There are 3 major types of pigment cells responsible for teleost color patterning: the black/gray melanophores, the yellow/reddish xanthophores and the blue/purple/white iridophores. In zebrafish these 3 types of pigment cells are fundamental for stripe formation, through run and chase cell–cell interactions (Watanabe and Kondo 2015). Recent studies on *Danio* pigment cells suggested that 2 groups of white pigment cells are critical for establishing pattern. White leucophores arises by trans-differentiation of adult melanophores. A second white cell type develops from a yellow-orange xanthophores or a xanthophore-like progenitor (Lewis et al. 2019). Similar studies in cichlids also demonstrated the importance of cell interactions in pigment patterning, even though the specific mechanisms might be different (O'Quin et al. 2013; Santos et al. 2014; Roberts et al. 2017; Kratochwil et al. 2018; Hendrick et al. 2019; Liang et al. 2020). Additionally, studies on rainbow trout suggested that homozygous mutation of an albinism gene, led to not only reduced number of melanophores, but also significantly larger size of xanthophores, which finally led to yellow-albino fish with golden color (Hattori et al. 2020). However, it remains to be further proved whether the change of the number, morphology and pigment synthesis of one type of pigment cells will also cause the corresponding change of the number, morphology and pigment synthesis of other pigment cells.

It has been acknowledged that 3 additional amino acids (9 bp insertion) in the *pmel* TM region caused premature cell death, which led to a dominant white plumage in farmed chicken (Kerje et al. 2004). This dominant negative allele has a much more severe effect on pigmentation than a complete loss-of-function allele (Watt et al. 2011). It is also worth mentioning that the *smoky* allele in chicken which was derived from the dominant white allele and represents a loss-of-function allele that partially rescue pigment synthesis (Kerje et al. 2004; Watt et al. 2011). In Japanese quail, this gene was also associated with the formation of yellowish plumage through GWAS mapping (Ishishita et al. 2018). In fish, the role of *pmel* in body color formation remains to be illustrated. Even though *pmela* has been acknowledged to be fundamental for melanin biosynthesis in larval zebrafish (Lahola-Chomiak et al. 2019), detailed role of

pmela and *pmelb* in teleost body color formation remains to be investigated. As a food fish farmed worldwide, tilapia has been favored for its strong resistance to disease, fast growth and high protein content. Tilapia is also an excellent model for scientific research because it has a published genome, short time to sexual maturity, short spawning cycle and large brood sizes. In a previous study, we developed the Nile tilapia as a model for studying teleosts color patterns, and identified severe vitiligo-like phenotypes in *pmel* F0 mutants, suggesting that *pmel* genes are indeed fundamental for tilapia body color formation (Wang et al. 2021). However, whether the homozygous mutation of *pmel* genes will give a healthy attractive white, silver, yellowish, golden body color or even a confusing mosaic pattern in tilapia still remains to be investigated.

In this study, we characterized the evolutionary history of the *pmela* and *pmelb* genes, and analyzed their expression in Nile tilapia. We then used CRISPR/Cas9 gene editing to disrupt *pmela* and *pmelb* and create homozygous mutants. We also analyzed the phenotype of these mutants to infer the function of *pmel* in this species. Disruption of PMEL yielded a complete golden body color in Nile tilapia, which was reflected by the changes of pigment cell numbers and cell sizes of melanophores and xanthophores. Our study provides a path to engineer a new strain of golden tilapia and might also deepen the understanding of pigment cell biology and color pattern formation in teleosts.

Materials and Methods

The founder strain of Nile tilapia was obtained from Prof. Nagahama (Laboratory of Reproductive Biology, National Institute for Basic Biology, Okazaki, Japan). This strain has been in laboratory culture for more than 20 years and is thus largely homozygous. Experimental tilapia were reared in recirculating aerated freshwater tanks and maintained at ambient temperature (27 °C) under a natural photoperiod. Prior to the experiments, the fish were kept in laboratory aquariums under 15:9 h light:dark conditions at temperature of 27 ± 1 °C for 11 week. All animal experiments conformed to the Guide for the Care and Use of Laboratory Animals and were approved by the Committee for Laboratory Animal Experimentation at Southwest University, China.

Identification of *pmel* Genes From Different Animal Species

We examined the genomes of 15 animal species (zebra cichlid *Maylandia zebra*, Nile tilapia *Oreochromis niloticus*, Japanese medaka *Oryzias latipes*, guppy *Poecilia reticulata*, torafugu *Takifugu rubripes*, channel cat fish *Ictalurus punctatus*, spotted gar *Lepisosteus oculatus*, zebrafish *Danio rerio*, tongue sole *Cynoglossus semilaevis*, coelacanth *Latimeria chalumnae*, common frog *Rana temporaria*, human *Homo sapiens*, house mouse *Mus musculus*, chicken *Gallus gallus* and common lizard *Zootoca vivipara*) to identify *pmel* genes in each species. These 15 species were representative animal species from fishes and also groups at different evolutionary positions. The genomic sequences of all species are available at the NCBI and Ensemble data base. They have relatively high quality genome sequences which allow us to isolate both *pmel* genes to reflect the true evolutionary history. All *pmel* genes were identified by tblastn ($E = 2 \times 10^{-5}$) against genome sequences, using zebrafish PMELA and PMELB proteins.

Phylogenetic Analyses and Genomic Distribution

We chose to use more conservative amino acids sequences, rather than nucleotide sequences for phylogenetic analyses. The amino acid sequences of *pmel* genes were aligned by ClustalW with default parameters using the multiple alignments of software BioEdit (Frolov et al. 1997). Phylogenetic trees were generated by the neighbor joining (NJ) method using the program MEGA6.0 software (Tamura et al. 2013). The final picture of NJ tree was modified with Adobe Illustrator CS6 (Adobe Inc. USA).

The Gene Functional Domain Prediction and Promoter Binding Site Analysis

The functional domain prediction of tilapia PMELA and PMELB was carried out in SMART online program. The 2k bp promoter sequences of *pmela* and *pmelb* were downloaded from the NCBI database. The cis-regulating elements of the promoter were predicted and analyzed in AnimalTFDB3.0 program, and the MITF binding consensus sequences were highlighted.

RT-PCR Validation of *pmela* and *pmelb* Expression

The *pmela*- and *pmelb*-specific primers used for reverse transcription PCR amplification were designed using Primer Premier 6. The sequences (*pmela*-RT-PCR-F/R and *pmelb*-RT-PCR-F/R) were listed in Table 1. Triplicate samples were collected at 2, 4, 6, 8, 10 dpf (whole fish) and 20, 30, 60, 90 dpf (skin) and adult stage (different tissues, including skin). Reverse transcription was conducted in a total reaction volume of 20 μL, which included 2 μg total RNA and 2 μL RT reaction mixture. For PCR amplification, *pmel* specific primers or *β*-actin primers were added into the reaction at the beginning of PCR and each PCR run for 34 cycles. The PCR products were separated by agarose gel electrophoresis and photographed under UV illumination.

Establishment of *pmela*$^{-/-}$, *pmelb*$^{-/-}$, and *pmela*$^{-/-}$;*pmelb*$^{-/-}$ Mutants by CRISPR/Cas9

We screened all exons of the 2 genes for potential/available target sites, but unfortunately, we only found the available sites in the fourth and third exon, respectively, but not in any other exons. Two gRNAs, targeting exon 4 of *pmela* and exon 3 of *pmelb*, were used to disrupt *pmela* and *pmelb* simultaneously in tilapia. The sequences of gRNA targets were CCCACCAAACCAGACGGTGCTCC and GGAAAAGTGACGTTTAATGTTGG, in which CCC and TGG were used as the PAM regions (Figure 2A–C and G–I). *Fsp*EI and *Tsp*45I respectively were used for enzymatic digestion of the amplified target regions. About 400 fertilized eggs were used for gene editing and 100 for control. The survival rate was nearly 95% after CRISPR.

The *pmela* and *pmelb* mutant fish with the highest indel frequency were used as G0 founders. They were raised to sexual maturity and mated with wild-type tilapia. F1 larvae were collected at 10 dah and genotyped by PCR amplification and subsequent *Fsp*EI and *Tsp*45I digestion.

CRISPR/Cas9 was performed to knockout *pmela* and *pmelb* in tilapia as described previously (Wang et al. 2021).

Table 1. Sequences of primers used in this study

Primer	Sequence (5′–3′)	Purpose
pmela-Cas9-F	CTTGACCTCTCCTTCCACATTTGAC	Positive gene knockout fish screening
pmela-Cas9-R	TGCTGCTAAGCTCTTATGGGG	Positive gene knockout fish screening
pmelb-Cas9-F	CCAAAAACCGCTTCACTCGTT	Positive gene knockout fish screening
pmelb-Cas9-R	TCTTCCTGTGGGGACTGACC	Positive gene knockout fish screening
pmela-page-F	AGCAAAAGCGGGCTTCACTA	F1 and F2 mutant fish screening
pmela-page-R	CCCCCTTGGTAAGGTTTCCT	F1 and F2 mutant fish screening
pmelb-page-F	ATTGTCCTGAATGAAGTATT	F1 and F2 mutant fish screening
pmelb-page-R	AGGTCAATAGTGAAGGTAACT	F1 and F2 mutant fish screening
pmela-RT-PCR-F	ATTGGACCGGAGTTTTCCCC	Validation of *pmela* expression
pmela-RT-PCR-R	GAGGCAACTACCACGACCTC	Validation of *pmela* expression
pmelb-RT-PCR-F	ACCCCTCATGGAACACCAAG	Validation of *pmelb* expression
pmelb-RT-PCR-R	CCCGAGCTGATGTAGGTGTG	Validation of *pmelb* expression
β-actin-F	GGCATCACACCTTCTACAACGA	Internal control
β-actin-R	ACGCTCTGTCAGGATCTTCA	Internal control
M13+	CGCCAGGGTTTTCCCAGTCACG	Sequencing and clone screening
M13-	AGCGGATAACAATTTCACACAG	Sequencing and clone screening

Briefly, the guide RNA and Cas9 mRNA were co-injected into one-cell-stage embryos at a concentration of 150 and 500 ng/μL, respectively. Twenty injected embryos were collected 72 h after injection. Genomic DNA was extracted from pooled control and injected embryos and used to access the mutations. DNA fragments spanning the target site for each gene were amplified using gene-specific primers (*pmela*-Cas-F/R and *pmelb*-Cas-F/R) listed in Table 1. The mutated sequences were analyzed by restriction enzyme digestion with *Fsp*EI and *Tsp*45I and Sanger sequencing.

Heterozygous F1 offspring were obtained by F0 XY male founders mated with WT XX females. The F1 fish were genotyped by fin clip assay and the individuals with frameshift mutations were selected. XY male and XX female siblings of F1 generation, carrying the same mutation, were mated to generate homozygous F2 mutants. Heteroduplex mobility assays were performed using polyacrylamide gel electrophoresis to detect the mutations, primer sequences (*pmela*-page-F/R and *pmelb*- page-F/R) used for mutants screening were listed in Table 1. The *pmela*$^{-/-}$, *pmelb*$^{-/-}$, and *pmela*$^{-/-}$;*pmelb*$^{-/-}$ mutants were confirmed using restriction enzyme digestion and Sanger sequencing. The genetic sex of each fish was determined by genotyping using sex-linked marker (marker 5) as described previously (Sun et al. 2014).

Image Recording and Pigment Cell Observation at Different Developmental Stages

Larvae fish at 5, 7, 12, and 30 dpf and early juvenile stage at 60 dpf were shifted to an observation dish with clean water, photographed by Olympus SZX16 stereomicroscope (Olympus, Japan) under bright or transparent field with different magnification. The 90 dpf wild-type and mutant fish were shifted to the same 15 × 5 × 15 cm^3 glass water tanks separately, before being photographed with a Nikon D7000 digital camera (Nikon, Japan) against a blue background. ACDSee Official Edition software (ACDSystems, Canada) and Adobe Illustrator CS6 (Adobe Inc. USA) were used to format the pictures.

Pigment Cell Analysis of the *pmela*$^{-/-}$, *pmelb*$^{-/-}$, and *pmela*$^{-/-}$;*pmelb*$^{-/-}$ Mutants

Larvae submerged in clean water at 7 and 12 dpf were photographed from the lateral view by Olympus SZX16 stereomicroscope (Olympus, Japan) under bright field. Caudal fin from fish at 60 and 90 dpf were photographed with a Nikon D7000 digital camera (Nikon, Japan) against a white background. The caudal fins were removed with medical scissors, soaked in 0.65% Ringers' solution and directly observed with Olympus SZX16 stereomicroscope (Olympus, Japan) without cover slip under transparent or bright field. Scales from fish at 60 and 90 dpf were soaked in 0.65% Ringers' solution under cover slip, and were observed under microscope (Germany, Leica EM UC7). Image recording of pigment cells was conducted as quickly as possible after putting them in the Ringers' solution as the preparations are not stable. ACDSee Official Edition software and Adobe Illustrator CS6 were used to format the pictures. To analyze the number of melanophores, 9 fish per group were anesthetized with tricaine methasulfonate (MS-222, Sigma–Aldrich, USA) and immersed in 10 mg/ml epinephrine (Sigma, USA) solution for 15 min to contract melanin. The sizes of the pigment cells and global pigmentation were measured using Image J software (Schneider et al. 2012). GraphPad Prism 5.01 software (Graphpad, USA) was used to analyze the differences in the numbers and sizes of melanophores in *pmela*$^{-/-}$, *pmelb*$^{-/-}$, and *pmela*$^{-/-}$;*pmelb*$^{-/-}$ mutants and wild-type fish. Data values (mean ± SD) were statistically evaluated by one-way ANOVA with Duncan's post hoc test and Student's *t*-test. $P < 0.05$ was considered to be statistically significant, as indicated by different letters above the error bar.

Results

Pmela and *pmelb* Diverged After the Teleost-Specific Genome Duplication

As shown in Figure 1, we found that euteleosts have 2 copies of *pmel* due to the third round of genome duplication, whereas nonbony fish and tetrapods have only one copy. Nile tilapia

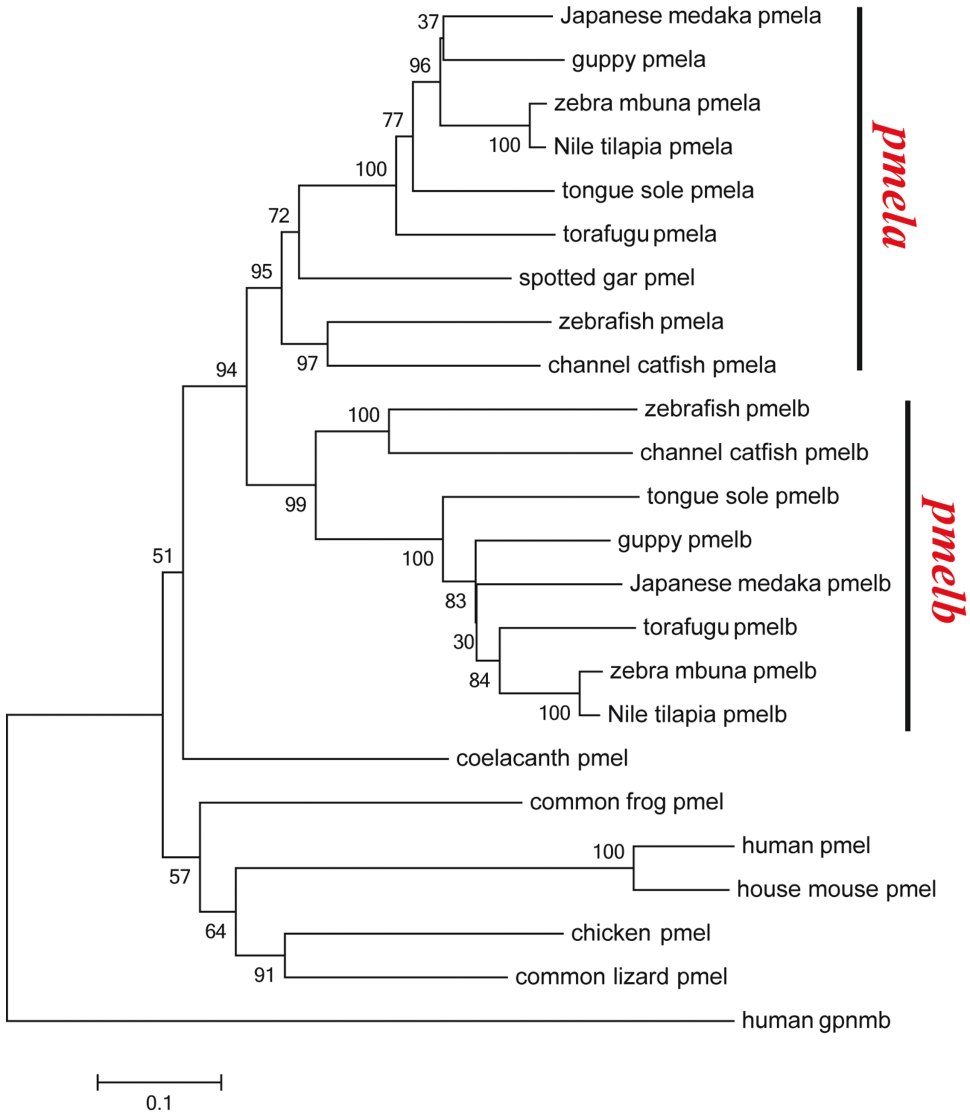

Figure 1. Phylogenetic tree of *pmel* genes from 15 representative species. The NJ method was used to construct the tree by MEGA6.0 software, using human GPNMB protein (the homologue of PMEL) as the out-group. The multiple alignments of software Bioedit was used to align the amino acid sequences. The *pmel* genes were divided into 2 branches: *pmela* and *pmelb*. Eubony fish have 2 copies due to the third round of genome replication, whereas nonbony fish and quadrupeds do not have 2 copies. The *pmel* amino acids were downloaded from zebra mbuna (XP_004545057 of *pmela* and XP_004560330 of *pmelb*, respectively), Nile tilapia (XP_019214528 of *pmela* and XP_003457123 of *pmelb*, respectively), Japanese medaka (XP_004069166 of *pmela* and XP_004071062 of *pmelb*, respectively), guppy (XP_008408226 of *pmela* and XP_008412883 of *pmelb*, respectively), torafugu (XP_029683274 of *pmela* and XP_029690408 of *pmelb*, respectively), channel cat fish (XP_017306583 of *pmela* and XP_017342597 of *pmelb*, respectively), spotted gar (XP_015199523), zebrafish (XP_021335225 of *pmela* and XP_691276 of *pmelb*, respectively), tongue sole (XP_024915820 of *pmela* and XP_008317243 of *pmelb*, respectively), coelacanth (XP_005986276), common frog (XP_040197009), human (NP_001186983), house mouse (XP_030100827), chicken (XP_040510678), and common lizard (XP_034959828).

pmela was most similar to the zebra cichlid, followed by Japanese medaka, guppy, and torafugu. The *pmelb* was also most similar to the zebra mbuna, followed by torafugu/tongue sole, guppy/Japanese medaka, and then other teleosts. The promoters of *pmela* and *pmelb* each contain several binding sites for *mitf*, consistent with the idea that both genes are directly regulated by *mitf* (Supplementary Figures S1 and S2). The closest paralog to PMEL is Glycoprotein Nonmetastatic Melanoma Protein B (GPNMB), another transmembrane glycoprotein also regulated by *mitf* (Loftus et al. 2009; Gutknecht et al. 2015).

Expression of *pmela* and *pmelb* in Nile Tilapia

RT-PCR analysis showed high levels of expression of both *pmela* and *pmelb* in eyes, skin, and whole embryos. Weak expression of *pmela* was detected in heart and testis, but it was rarely expressed in other tissues (Supplementary Figure S3) (Brawand et al. 2014). Some expression of *pmelb* was detected also in brain and fins (Supplementary Figure S4). Across the different developmental stages (2, 4, 6, 8, 10, 20, and 30 dpf of the whole fish, 60, 90 dpf and adult of the black skin) of wild-type Nile tilapia, *pmela* and *pmelb* were detected with similar expression levels and trends at all stages. They were highly expressed at 4, 6, 8, 10, and 90 dpf, but showed less expression at 20, 30, 60 dpf and the adult stage. Neither gene was expressed at the 2 dpf blastula stage, probably because pigmentation genes are only expressed after neural crest cells (NCCs) are specified. Additionally, *pmela* and *pmelb* were consistently expressed in whole fish

from 4 to 10 dpf, with the highest expression at 8 and 10 dpf (Supplementary Figure S5). This was inconsistent with the observation of several waves of melanophore increase in our previous study, including key events at 5 dpf (the time melanophores spread on the yolk sac), 7 dpf (the time melanophores spread on both the trunk and the yolk sac), 12 dpf (the time melanophores spread across the whole trunk but are not detected in the fins), and 90 dpf (the time vertical bar patterns began to form in both trunk and fins) (Wang et al. 2021).

Establishment of the *pmela*$^{-/-}$, *pmelb*$^{-/-}$, and *pmela*$^{-/-}$;*pmelb*$^{-/-}$ Mutants in Tilapia

F0 founders were screened by restriction enzyme digestion and Sanger sequencing (Figure 2B, C, H, and I). The *pmela* and *pmelb* mutant fish with a high mutation rate (over 75%) were raised to sexual maturity and mated with wild-type tilapia to create F1 fish. In the *pmela* and *pmelb* F0 chimeras, various levels of hypopigmentation were observed in body and the iris was also hypopigmented, as we previously reported (Wang et al. 2021). These results indicated that the 2 genes are fundamental for body color formation and eye pigmentation in tilapia, and are probably necessary for melanin synthesis in all melanophores (NCC-derived and optic-cup derived melanophores).

The F1 mutant fish were obtained by crossing an F0 XY male with a wild-type XX female. We chose F0 XY male as founder fish to accelerate the establishment of mutant strain because males grow faster and get mature (150 dpf) earlier than females (240 dpf). Heterozygous *pmela* F1 offspring with a −5 bp deletion in the fourth exon were selected to breed the F2 generation (Figure 2C–E). Likewise, heterozygous *pmelb* F1 offspring with a −7 bp deletion in the third exon were selected to breed an F2 generation (Figure 2I–K). Finally, *pmela;pmelb* F2 were produced by mating a male *pmela* −5 bp F1 heterozygous mutant with a female −7 bp F1 *pmelb*-positive fish, then heterozygous *pmela;pmelb* F2 offspring with a −5 bp deletion in *pmela* and −7 bp deletion in *pmelb* were selected to breed the F3 generation (Supplementary Figure S6). A heteroduplex

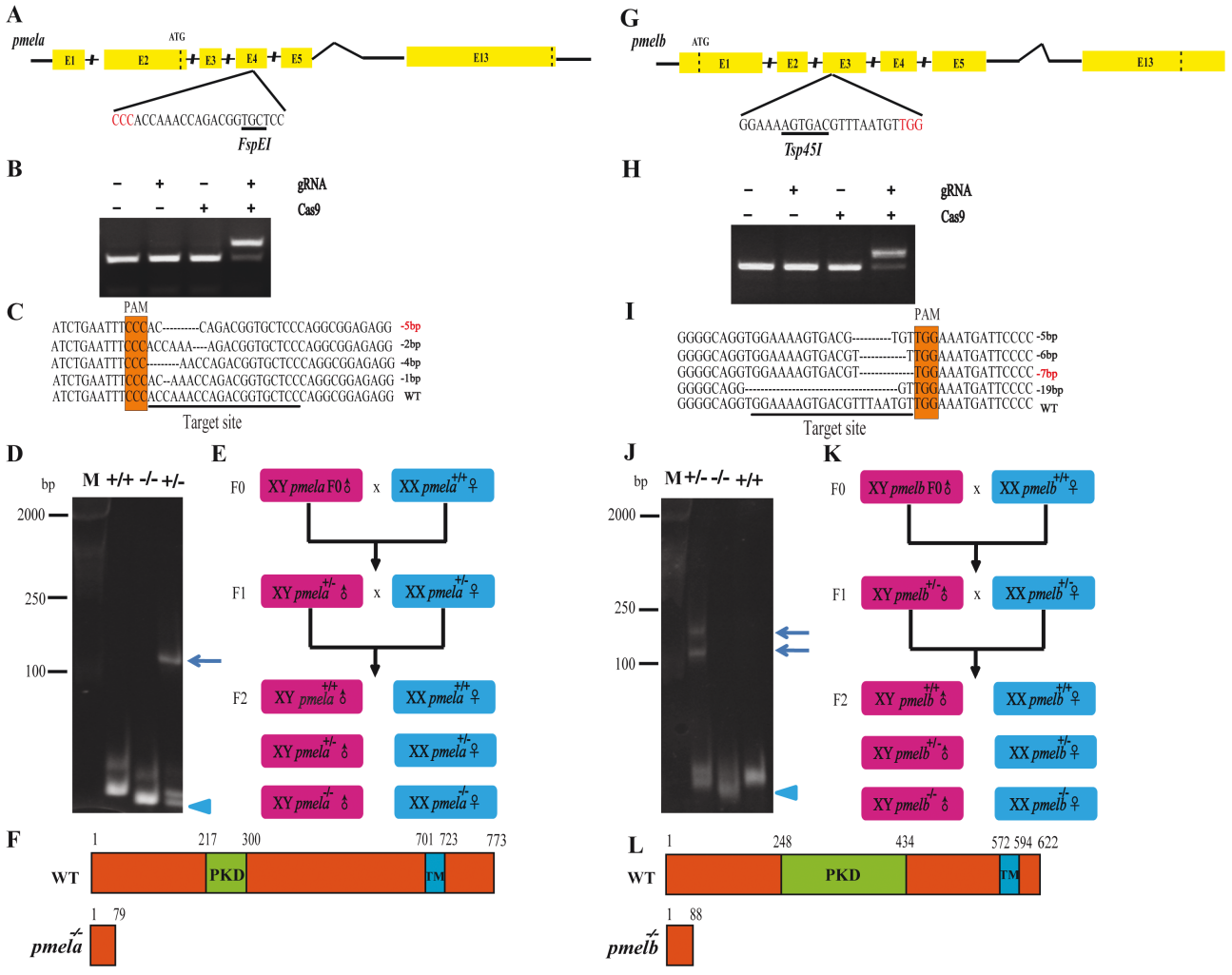

Figure 2. Establishment of *pmela*−/− (A–F) and *pmelb*−/− (G–L) mutant lines. (A, G) Gene structures of *pmela* and *pmelb* showing the target site and the *Fsp*EI and *Tsp*45I restriction site, respectively. (B, H) Restriction enzyme digestion of the amplified fragment of *pmela* and *pmelb* using primers spanning the target sites. The Cas9 mRNA and gRNA were added as indicated. (C, I) Sanger sequencing results from the uncleaved bands were listed. The PAM is marked in orange. Deletions are marked by dashes (–) and numbers to the right of the sequences indicate the loss of bases for each allele. WT, wild type. (D, J) Identification of *pmela* and *pmelb* F2 genotypes by hetero-duplex motility assay. Arrowheads show homo-duplexes and arrows show hetero-duplexes. (E, K) Schematic diagram showing the breeding. Plans of *pmela* and *pmelb* F0 to F2 fish. (F, L) Tilapia *pmela* and *pmelb* showing the functional domains (orange) including PKD domain (green) and TM domain (blue).

mobility assay identified the heterozygous *pmela*$^{+/-}$, *pmelb*$^{+/-}$, and *pmela*$^{+/-}$;*pmelb*$^{+/-}$ individuals as those possessing both heteroduplex and homoduplex amplicons vs. the *pmela*$^{+/+}$ and *pmela*$^{-/-}$ individuals with only homoduplex amplicons (Figure 2D and J). Nineteen of the 307 F2 fish were complete golden tilapia (*pmela*$^{-/-}$;*pmelb*$^{-/-}$ ~1/16), which was in line with Mendelian's law.

Melanophore Size, Number, and Melanin Biosynthesis Were Decreased in *pmel* Mutants

Several waves of increase in melanophore number were detected in wild-type tilapia, during which melanophore populations increased to pattern the whole fish (Wang et al. 2021). Like the tetrapods, melanophores in teleosts were also able to release melanosomes extracellularly (Supplementary Figure S7). We chose to analyze the melanophores of wild-type and *pmel* mutant fish at 7 dpf, shortly after melanophores first appear on the embryo and spread on both the yolk sac and the trunk. The wild-type fish had many well-pigmented macro-melanophores and normal sized melanophores on the head from 7 dpf (Figure 3A and A'). However, pigmented melanophores were greatly reduced in the *pmela*$^{-/-}$ (Figure 3B' and B') and *pmela*$^{-/-}$;*pmelb*$^{-/-}$ mutants (Figure 3D and D'). The remaining melanophores were unable to synthesis mature melanosomes, and most of the melanosomes were in phase II. The remaining macro-melanophores were light gray, a hypopigmented phenotype (Figure 3A, A', D, and D'). In contrast, although the *pmelb*$^{-/-}$ mutants also had fewer melanophores, some melanophores were still able to develop dark, mature melanosomes (Figure 3C and C'). The number of melanophores in *pmela*$^{-/-}$;*pmelb*$^{-/-}$ and *pmela*$^{-/-}$;*pmelb*$^{-/-}$ mutants was significantly lower than that of the wild-type fish. Although *pmelb*$^{-/-}$ mutants retained more melanophores, most of the pigmented melanophores were fragmented or found in a state of pigment-aggregation. The *pmela*$^{-/-}$;*pmelb*$^{-/-}$ double mutants had significantly reduced melanophore numbers and sizes compared with both wild-type fish and the single gene mutants (Figure 3E and F). Additionally, xanthophores were detected in significantly higher numbers and larger sizes than the wild-type fish at 12 dpf, which gave the fish a yellowish head (Figure 4A–C). This phenomenon probably could explain the complete golden color of the whole fish at later stages.

Xanthophore Number and Size Were Increased in *pmel* Mutants

In our previous study, we found that in wild-type fish xanthophores arose at 6 dpf, and sharply increased in number by 12 dpf (Wang et al. 2021). We used 12 dpf wild-type, *pmela*$^{-/-}$, *pmelb*$^{-/-}$, and *pmela*$^{-/-}$;*pmelb*$^{-/-}$ mutants to

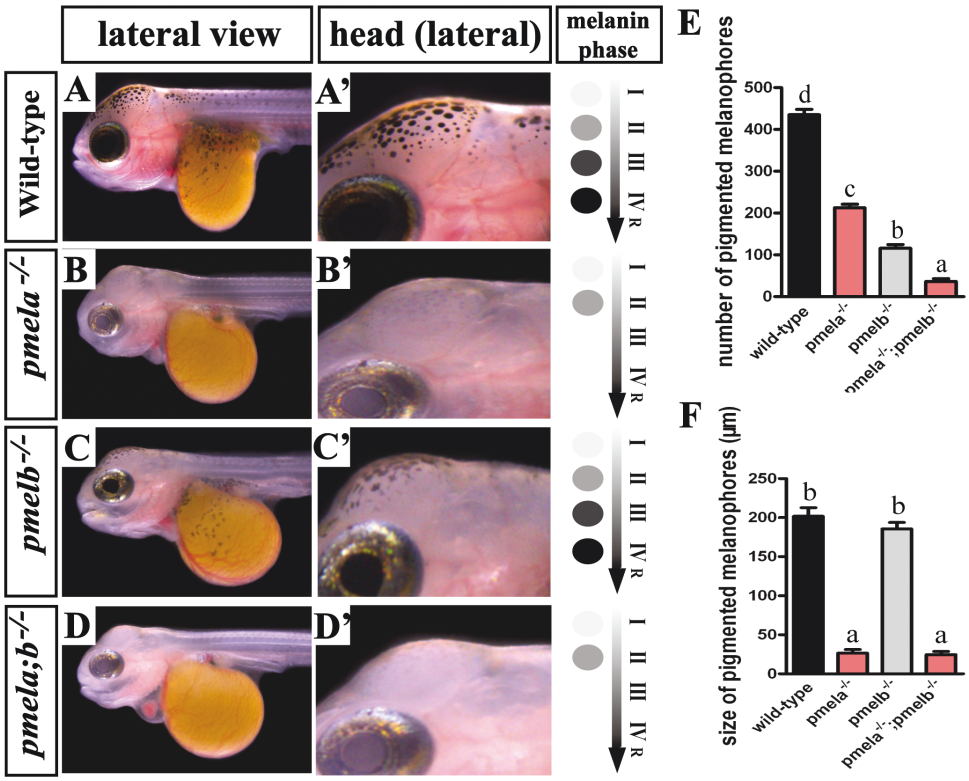

Figure 3. Mutation of *pmela* and *pmelb* resulted in significant melanophores reduction, cell size decrease, and melanin biosynthesis degeneration at 7 dpf. In *pmela*–/– and *pmela*–/–;*pmelb*–/– mutants, the melanophores were heavily reduced, but the remaining melanophores (mainly macro-melanophores) still kept the stretch like outlooks, and every one of them displayed hypopigmentation. Most of the melanin was in stage II. In wild-type fish and *pmelb*–/– mutants, the melanophores were capable of biosynthesizing mature melanin until stage IV, and then release to further patterning the whole fish. And the melanophores in *pmelb*–/– mutants were also heavily reduced when compared with the wild-type fish. The pigmented melanophores on the kept decrease from *pmela*–/––*pmelb*–/––*pmela*–/–;*pmelb*–/– mutants, and the difference was significant ($P < 0.05$). However, when related to the size of melanophores, there was no such an orderly decrease. The size of *pmela*–/– and *pmela*–/–;*pmelb*–/– mutants were significantly smaller than that of *pmelb*–/– and wild-type fish. The single melanophore was unable to synthesize much melanin due to the size reduction and PMEL disruption. Data are expressed as mean ± SD ($n = 9$). Significant differences in the data between groups were tested by one-way ANOVA and Duncan's post hoc test. $P < 0.05$ was considered to be statistically significant, as indicated by different letters above the error bar. R, release.

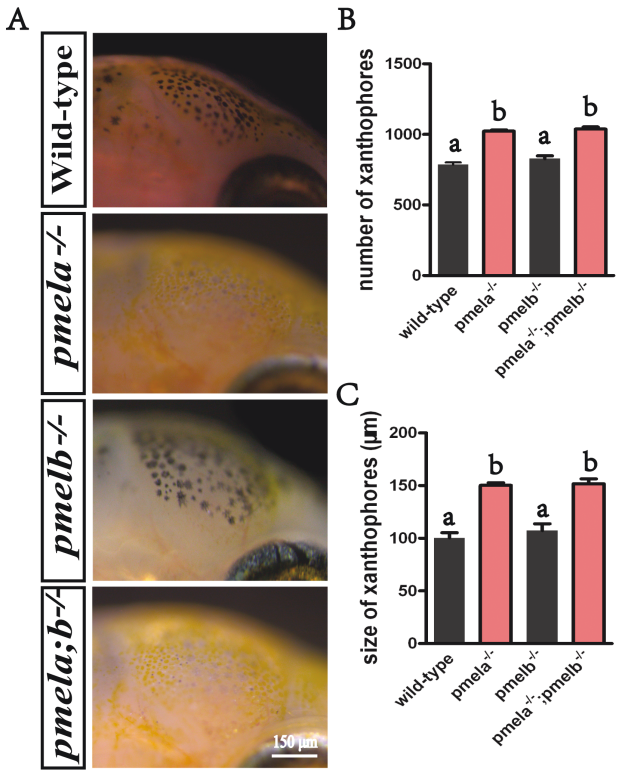

Figure 4. Mutation of *pmela* and *pmelb* resulted in melanophores reduction, melanin biosynthesis degeneration, more and larger sized xanthophores on the head at 12 dpf. (A) Mature melanin inside the functional stretch-like melanophores was easily detected in the wild-type fish at 12 dpf. However, the light gray melanophores with serious hypopigmentation were detected in the head of *pmela–/– and pmela–/–;pmelb–/–* mutants, the melanin inside were almost all in phase I or II so far. Thus melanophores were unable to biosynthesis mature melanin to further pattern the whole fish. Additionally, melanophores were heavily reduced. As a contrast, more and larger sized xanthophores were detected, which made the head a golden outlook. (B and C) The number of xanthophores in *pmela–/–* and *pmela–/–;pmelb–/–* mutants were significantly higher than that of *pmelb–/–* and wild-type fish, and the size of xanthophores in *pmela–/–* and *pmela–/–;pmelb–/–* mutants were significantly lager than that of *pmelb–/–* and wild-type fish. Data are expressed as mean ± SD (n = 5). Significant differences in the data between groups were tested by one-way ANOVA and Duncan's post hoc test. $P < 0.05$ was considered to be statistically significant, as indicated by different letters above the error bar.

analysis xanthophore number and size in PMEL disrupted fish. The *pmela*$^{-/-}$ and *pmela*$^{-/-}$;*pmelb*$^{-/-}$ mutants showed significantly more and larger sized xanthophores, which was a major reason for the yellowish color of those mutants (Figure 4A–C). In wild-type fish, the xanthophores were often in a pigment-aggregated state, with a much smaller size than the expanded melanophores (Wang et al. 2021). However, in the *pmela*$^{-/-}$ and *pmela*$^{-/-}$;*pmelb*$^{-/-}$ mutants, the lateral top of the heads showed lots of yellow pigmentation, the xanthophores were filled with pteridines/carotenoids, and the sizes were much larger than wild-type fish and *pmelb*$^{-/-}$ mutants. The remaining melanophores were small and hypopigmented with small sizes, similar to the 7 dpf mutants (Figure 4A). These results indicated that loss of pigment biosynthesis function in melanophores led to decreased melanophore number and size, and a corresponding increase in xanthophore size and number.

RPE, Iris Pigmentation, and Eye Development Were Affected in *pmela* Mutants, Whereas Only Iris Pigmentation Was Affected in *pmelb* Mutants

Reduced eye pigmentation was observed in all developmental stages of *pmel* mutants, and the *pmela*$^{-/-}$ and *pmela*$^{-/-}$;*pmelb*$^{-/-}$ mutants were free of melanin in the eyes at early larvae stages (before 60 dpf). Thus fish at 60 and 90 dpf were used as materials for studying eye pigmentation and development. Pigmentation in the eyes (including both iris and RPE) displayed significant differences between the mutants and wild-type fish. The *pmela*$^{-/-}$ and *pmela*$^{-/-}$;*pmelb*$^{-/-}$ mutants showed significant hypopigmentation in eyes, the RPE was dark red, and the iris was golden (Figure 5B and D). In contrast, the wild-type fish and *pmelb*$^{-/-}$ mutants had a black RPE, and a normally pigmented iris (Figure 5A and C). The development of eyes was also altered in *pmela*$^{-/-}$ and *pmela*$^{-/-}$;*pmelb*$^{-/-}$ mutants. Around 1/3 of both *pmela*$^{-/-}$ and *pmela*$^{-/-}$;*pmelb*$^{-/-}$ mutants had both serious reduction of iris iridescent-white pigmentation and significant eye abnormal development. Pigment deposition onto the inner surface of the cornea causes the appearance of the Krukenberg spindle. The area of iris covered by melanin stuck to the cornea was around 1/3 compared with the central black RPE area (Figure 5B', D', and E). Even though slow restoration of RPE pigmentation was detected at 90 dpf, part of the RPE area still had a blood red color indicative of insufficient melanin, and the Krukenberg spindle phenotype was durable (Figure 5E). In contrast, the wild-type fish and *pmelb*$^{-/-}$ mutants showed no significant abnormalities of eye development (e.g., pigment stuck to the cornea), even though the *pmelb*$^{-/-}$ mutants hypopigmentation of the eyes. The results of global pigmentation in eyes were consistent with the phenotype we showed above (Figure 5F).

Melanophore Number and Melanin Synthesis Were Restored in Older *pmela*$^{-/-}$ and *pmela*$^{-/-}$;*pmelb*$^{-/-}$ Mutants

Phenotypic analysis of the caudal fins suggested that pigmented melanophores increased with age in the mutants. The *pmela*$^{-/-}$ and *pmela*$^{-/-}$;*pmelb*$^{-/-}$ mutants had only a few pigmented melanophores before 60 dpf. However, after further development, small pigmented melanophores were observed in the *pmel* mutants. The caudal fins in wild-type, *pmela*$^{-/-}$, *pmelb*$^{-/-}$ and *pmela*$^{-/-}$;*pmelb*$^{-/-}$ mutants were used as samples to study the repigmentation and repatterning progress of melanophores. In wild-type fish at 60 dpf, hyperpigmented bars separated by light colored interbars were observed in the caudal fin (Figure 6A). Melanophores were detected in large numbers in the hyperpigmented bar regions (Figure 6A'). In *pmela*$^{-/-}$ mutants at 60 dpf, yellowish caudal fins without any bars were detected (Figure 6B). No pigmented melanophores were detected at this time period. What was striking was that aggregated iridescent purple guanine was detected in cells with branching-like-clusters sharing a shape and size similar to melanophore, both in caudal fins and even scales (Figure 6B' and Supplementary Figure S8). We suggest that melanophores under specific conditions (melanin-free or melanin biosynthesis deficient) were able to synthesize or accumulate guanines. In *pmelb*$^{-/-}$ mutants at 60 dpf, no obvious bars but some pigmented melanophores were detected in the caudal fins (Figure 6C and C'). In *pmela*$^{-/-}$;*pmelb*$^{-/-}$ mutants at 60 dpf, the whole

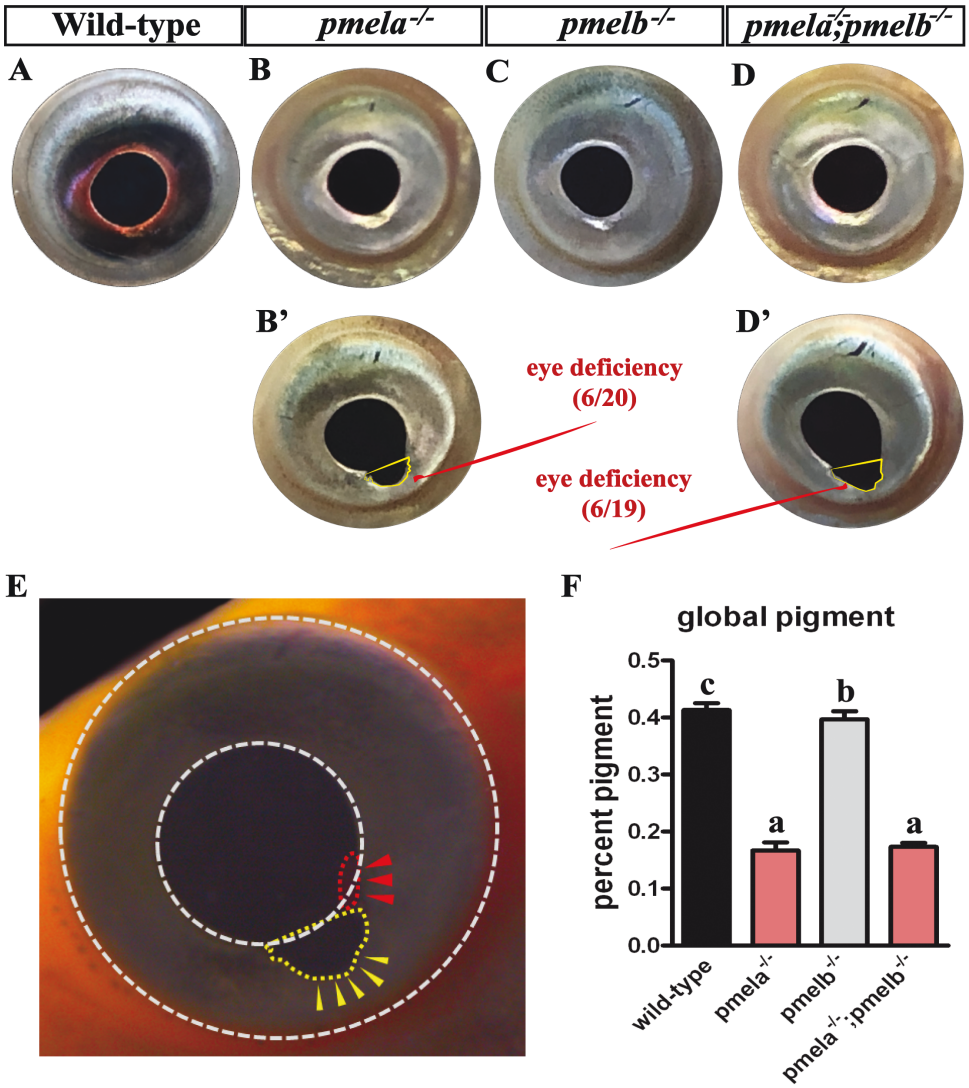

Figure 5. Mutation of *pmela* resulted in RPE hypopigmentation and eye deficiency at 60 and 90 dpf. (A–D) The *pmela*–/– and *pmela*–/–;*pmelb*–/– mutants showed deep red color in RPE, but difficult to be distinguished from the lateral view. While deep black color was detected in the RPE of wild-type fish and *pmelb*–/– mutants. No black pigmentation was detected in the iris of *pmela*–/– and *pmela*–/–;*pmelb*–/– mutants, but some black pigmentation was detected in the iris of *pmelb*–/– mutants. (B' and D') Additionally, the *pmela*–/– (6/20) and *pmela*–/–;*pmelb*–/– (6/19) mutants were detected with serious eye deficiency (ocular pigment dispersion and pigmentary glaucoma) in around 1/3 mutants, compared with wild-type fish and *pmelb*–/– mutants at 60 dpf. (E) Around 1/3 of the *pmela*–/– and *pmela*–/–;*pmelb*–/– mutants were detected with abnormal eye development at 90 dpf, reflected by some melanin spread out of the round iris (yellow dashed box highlighted by yellow arrow heads). Additionally, even though slow restoration of melanin biosynthesis was observed with individual development, a part of the RPE and iris area was detected with almost no melanin, reflected by blood red color (red dashed box highlighted by red arrow heads, under strong bright field). Generally, this is a phenotype of Krukenberg spindle (pigment stuck to the cornea). (F) The statistical analysis of eye pigmentation, the percentages of *pmela*–/– and *pmela*–/–;*pmelb*–/– mutants were significantly lower than in *pmelb*–/– mutants and wild-type fish ($P > 0.05$). And there was also significant difference between *pmelb*–/– mutants and wild-type fish ($P < 0.05$). Data are expressed as mean ± SD ($n = 9$). Significant differences in the data between groups were tested by one-way ANOVA and Duncan's post hoc test. $P < 0.05$ was considered to be statistically significant, indicated by different letters above the error bar.

fins were yellowish without bars, and many purple-guanine-pigmented melanophores were detected randomly spread across the whole fins (Fig. 6D and D'). At 90 dpf, a significant increase in pigmented melanophores was detected in the caudal fin of wild-type fish (Figure 6E). Additionally, many red erythrophores/xanthophores were detected in the fins (Figure 6E'). In *pmela*$^{-/-}$ mutants at 90 dpf, a significant increase in small melanophores was detected across the whole fins, and they spread evenly across the fin (Figure 6F). Large numbers of evenly distributed white iridophores were also detected (Figure 6F'). In *pmelb*$^{-/-}$ mutants at 90 dpf, increased numbers of melanophores were detected in the caudal fins, with larger size and significant higher number than the *pmela*$^{-/-}$ mutants at the same developmental stage (Figure 6G). Additionally, the white iridophores also increased compared with the wild-type fish, similar to the situation revealed in *pmela*$^{-/-}$ mutants. In *pmela*$^{-/-}$;*pmelb*$^{-/-}$ double mutants at 90 dpf, melanophores were also more abundant compared to the 60 dpf *pmela*$^{-/-}$;*pmelb*$^{-/-}$ mutants. The melanophores in the double mutants were in spot-like small size, and fewer in number than in wild-type, *pmela*$^{-/-}$ and *pmelb*$^{-/-}$ mutants at the same stage. Interestingly, the number of red erythrophores/xanthophores increased in the double mutants, which contributes to a more yellowish

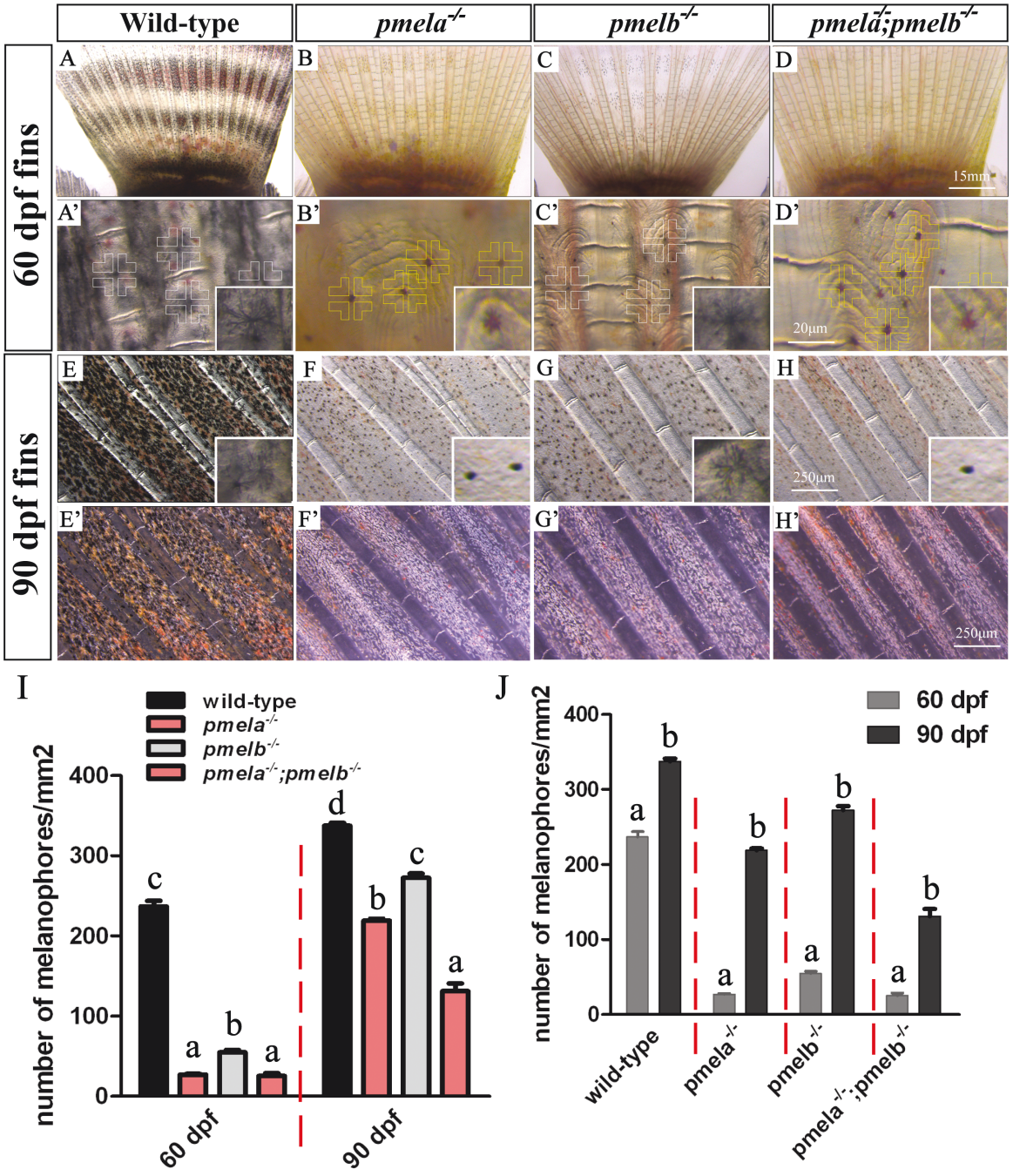

Figure 6. Mutation of *pmela* and *pmelb* resulted in melanophores reduction at 60 dpf, but with some restoration at 90 dpf in caudal fins. (A, A', E, and E') Large number of melanophores, erythrophores, and xanthophores were observed in 60 and 90 dpf wild-type caudal fin. Obvious black vertical bars and light pigmented interbars were also detected in wild-type fish, the melanophores with branch like clusters (white cross) were in a higher density in bars than in interbars. (B, B', F, and F') Almost no pigmented melanophores were detected in the caudal fins of *pmela*–/– mutants at 60 dpf, but xanthophores were detected. Some guanine filled in the not fully pigmented melanophores, thus making it showing branching-like clusters with red and purple colors (golden cross). The pigmented melanophores were detected with spot-like shape in 90 dpf *pmela*–/– mutants. The iridophores were most in white color, and many xanthophores were also detected. Both the latter 2 types of pigment cells were widely distributed between the fin rays. (C, C', G, and G') A few pigmented melanophores were detected in the fins of *pmelb*–/– mutants at 60 dpf, with branching-like clusters. Many iridophores and xanthophores were also detected. More pigmented melanophores were detected in *pmelb*–/– mutants at 90 dpf than at 60 dpf. All these melanophores were in a smaller size than the wild-type melanophores, but larger than in *pmela*–/– mutants. Additionally, xanthophores and iridophores were detected with the similar color patterning with *pmela*–/– mutants at the same developmental stage. (D, D', H, and H') Completely no pigmented melanophores were detected in the caudal fins of *pmela*–/–;*pmelb*–/– mutants. While many iridophores were observed to be filled in the not pigmented melanophores, thus showing red and purple colors (golden cross). Significant less melanophores than wild-type, *pmela*–/–, and *pmelb*–/– mutants were detected in the fins of *pmela*–/–;*pmelb*–/– mutants at 90 dpf. (I) In 60 dpf wild-type, *pmela*–/–, *pmelb*–/–, and *pmela*–/–;*pmelb*–/– caudal fins, the pigmented melanophores in *pmela*–/– and *pmela*–/–;*pmelb*–/– were significantly lower than in *pmelb*–/– mutants and wild-type fish. While the pigmented melanophores in *pmelb*–/– mutants were also significantly lower than the wild-type fish. In 90 dpf wild-type, *pmela*–/–, *pmelb*–/–, and *pmela*–/–;*pmelb*–/– caudal fins, the pigmented melanophores in *pmela*–/–;*pmelb*–/– mutants were significantly lower than in *pmela*–/– mutants, the pigmented melanophores in *pmela*–/– mutants were significantly lower than in *pmelb*–/– mutants, and the pigmented

or reddish body color (Figure 6H and H'), and the whole fish were seriously hypopigmented compared to the wild-type fish (Supplementary Figure S9). Statistical analysis of the melanophores of the *pmel* mutants and wild-type fish at 60 and 90 dpf was consistent with the descriptions above (Figure 6I and J). The restoration of melanin biosynthesis in *pmela*$^{-/-}$ and *pmela*$^{-/-}$;*pmelb*$^{-/-}$ mutants at older ages indicated that additional pathways might be involved in melanin biosynthesis.

Body Color of *pmel* Mutants at Different Developmental Stages

We characterized the phenotype of the mutant fish in their early developmental stages. At 12 dpf, wild-type fish showed no bars, and melanophores were spread evenly across the whole trunk (Figure 7A). At 60 dpf, wild-type fish showed black bars separated by light colored interbars. A higher density of melanophores was detected in the bar regions. Iridophore number sharply increased in the interbar regions (Figure 7B). At 90 dpf, wild-type fish showed strong black bars separated by iridescent interbars (Figure 7C and C'), much like the 150 dpf and adult fish (Figure 7M).

At 12 dpf, the *pmela*$^{-/-}$ mutant fish showed serious hypopigmentation across the whole fish (including RPE). Melanophore numbers were reduced on the trunk surface, and the remaining melanophores were light gray, indicative of a reduction in melanin synthesis (Figure 7D). Almost no pigmented melanophores were observed in the mutants at 60 dpf (Figure 7E). Hypopigmented patterns on the dorsal fin and a red-black RPE were observed in the lateral view (Supplementary Figure S10). At 90 dpf, the body color was yellowish, and the iris showed obvious hypopigmentation (Figure 7F and F').

At 12 dpf, *pmelb*$^{-/-}$ mutant fish showed hypopigmentation but with more pigmented melanophores than the *pmela*$^{-/-}$ mutant fish (Figure 7G). At 60 dpf, melanophores were present in reduced numbers on the trunk surface, and although regular bars were not seen, we occasionally detected irregular patches of pigmentation (Figure 7H). At 90 dpf, the fish showed yellowish body color with slightly pigmented dorsal patches compared with the *pmela*$^{-/-}$ mutant fish (Figure 7I and I').

At 12 dpf, *pmela*$^{-/-}$;*pmelb*$^{-/-}$ double mutants showed a phenotype similar to the *pmela*$^{-/-}$ mutants. The RPE and the trunk were hypopigmented. Macro-melanophores with reduced melanin content were observed, but no pigmented melanophores were observed on the trunk (Figure 7J). At 60 dpf, no bars or pigmented melanophores were detected in the double mutants. They showed even more significant hypopigmentation compared with the *pmela*$^{-/-}$ or *pmelb*$^{-/-}$ mutants, which gave the whole fish a golden color (Figure 7K). At 90 dpf, significant hypopigmentation was detected in the double mutants. No bars or black/gray patterns were detected in the trunk and all the fish showing completely golden color. The iris was hypopigmented, but it was difficult to distinguish the differences of RPE pigmentation between the mutants and the wild-type fish from the lateral view (Figure 7L and L'). At 150 dpf, the double mutants showed a golden color with reddish fins, and the yellow pigmentation and remaining melanophores were spread evenly across the whole fish. The RPE was as black as the wild-type fish (Figure 7N).

Pigment Cell Number, Morphology, and Location Were Greatly Changed in *pmel* Mutants

The thin and partially transparent scales as skin appendages provided us excellent materials to investigate the cell number, morphology and location between each type of pigment cells. The 60 dpf (before melanin biosynthesis partially restored) and 150 dpf (melanin gradually accumulate over many weeks) scales of wild-type fish and *pmela*$^{-/-}$;*pmelb*$^{-/-}$ double mutants were used as materials to reveal the relative pigment cell number, morphology and location between the wild-type fish and PMEL-free golden fish. Just as predicted, the number and sizes of melanophores and xanthophores were consistent with the results we showed above in different developmental stages. In wild-type fish, many melanophores were healthy and heavily pigmented with mature melanin, the dendrites were active and fully spread, which made a large branched cell, especially in the older 150 dpf melanophores. Additionally, iridophores were spread mainly on the surface of the mainly body of melanophores. However, the xanthophores were detected with a smaller, round shape. They located near the dendrites of melanophores, or even further away, probably restricted and rejected by melanophores (Figure 8A and C). As a contrast, in scales of 60 dpf PMEL-free hypopigmented fish, the melanophores with insufficient melanin biosynthesis were often detected with melanin-free melanophores filled with iridescent purple, blue or even red guanine, in both the main body and the dendrites of melanophores (Figure 8B). In the scales of older 150 dpf PMEL-free golden fish, the small number of melanophores detected had a tiny-spot appearance, and the gradually accumulated melanin gathered as a weak spots, with a much smaller size than that of the wild-type melanophores. Additionally, the xanthophores were obviously enlarged with "airenemes" in the mutants compared with those of the wild-type. The larger sizes of xanthophores allowed the mutants to produce more yellow pteridines/carotenoids. Besides, the xanthophores located near the melanophores, and some of them even clung on the main body of the tiny-spot-like melanophores, indicating that the nearest-neighboring distances between the melanophores and xanthophore were probably reduced and the interactions of them were heavily influenced. The remaining iridophores were arranged in a line between the weak melanophores, and eventually combined into a fish net structure in the scales (Figure 8D). These results suggested that the cell–cell interactions between the pigment cells (both the same type and different types of pigment cells) were altered in the PMEL-free golden fish. The relative pigment cell number, morphology and location (mainly between the melanophores and xanthophores) were completely different between the wild-type and mutants,

melanophores in *pmelb*–/– mutants were significantly lower than in wild-type fish. (J) The pigmented melanophores in 60 dpf wild-type, *pmela*–/–, *pmelb*–/–, and *pmela*–/–;*pmelb*–/– mutants were significantly lower than the wild-type fish and mutants at 90 dpf stage, respectively. Data shown in Figure 6I and J are expressed as the mean ± SD (n = 9). Significant differences in the data between groups were tested by one-way ANOVA and Duncan's post hoc test and Student's t-test, respectively. $P < 0.05$ was considered to be statistically significant, indicated by different letters above the error bar.

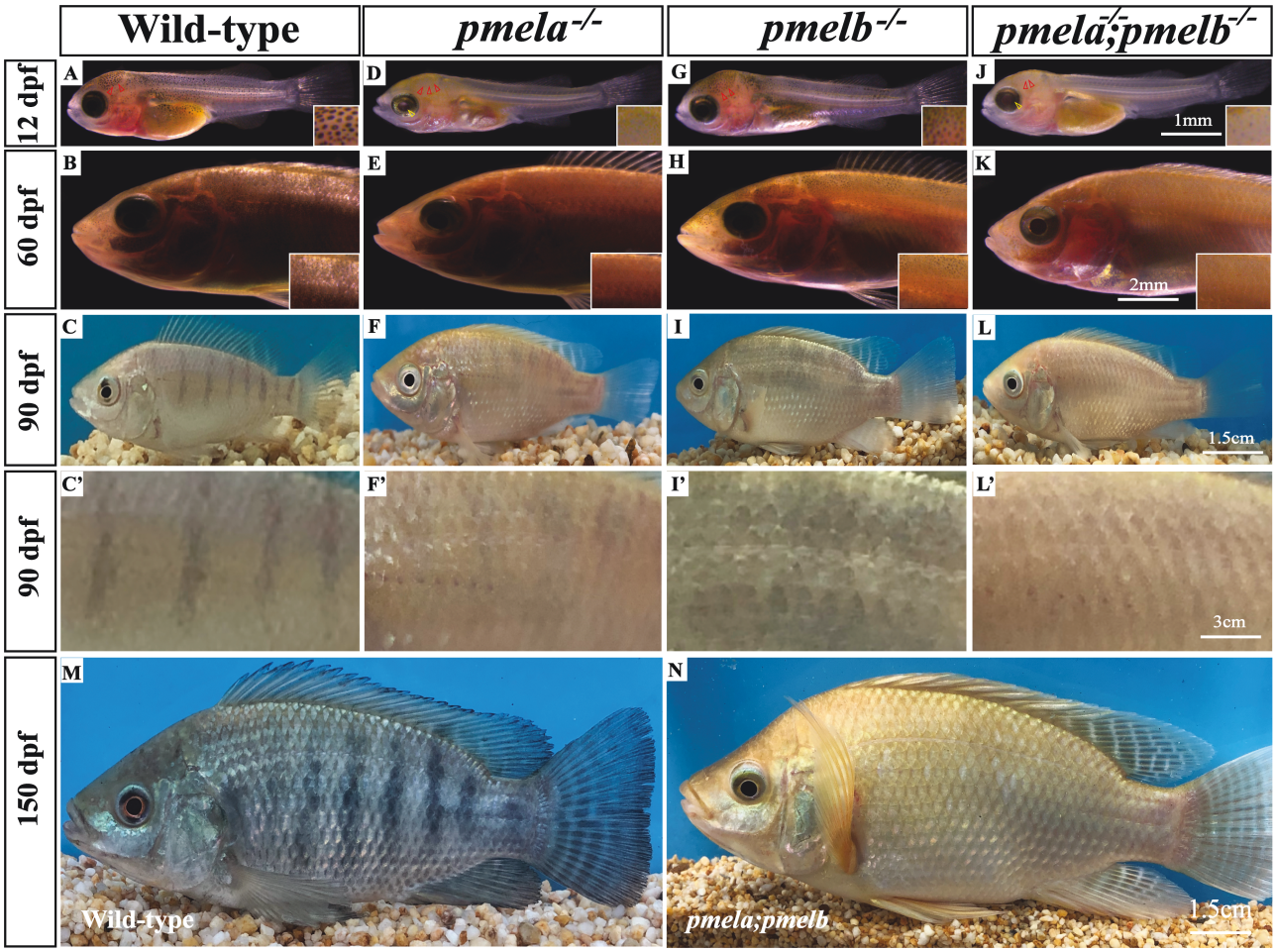

Figure 7. Mutation of *pmela* and *pmelb* resulted in serious hypopigmentation. The fish were checked at 12, 60, 90, and 150 dpf. Hypopigmentation of *pmela*–/–, *pmelb*–/–, and *pmela*–/–;*pmelb*–/– mutants were observed in trunk at all the developmental stages. (A) No bars were observed (the bars usually begin to appear at around 35 dpf) in wild-type fish. (B) Black wild-type fish with heavily pigmented vertical bars detected on the trunk at 60 dpf. (C and C') Wild-type fish with obvious vertical bars detected on the trunk at 90 dpf. (D) *pmela*–/– mutants with significant reduction of pigmented melanophores detected in whole fish at 12 dpf. Melanophores in the head and RPE were detected with significant hypopigmentation. (E) *pmela*–/– mutants with serious hyperpigmentation detected in trunk at 60 dpf. No obvious vertical bars were detected at this stage, the body color was evenly detected in the whole fish. Many gray iridophores were detected on the trunk. (F and F') *pmela*–/– mutants with hypopigmentation detected in whole fish, which made the fish show light golden body color at 90 dpf. (G) *pmelb*–/– mutants with hypopigmentation on trunk, while not on melanophores at 12 dpf. (H) *pmelb*–/– mutants with some pigmented melanophores detected in trunk and fins, but many of the melanophores were in abnormal states at 60 dpf. (I and I') *pmelb*–/– mutants detected with some black patterns which were different with the bars of wild-type fish at 90 dpf. The whole fish showed hypopigmentation. (J) *pmela*–/–;*pmelb*–/– mutants detected with even more significant hypopigmentation than *pmela*–/– and *pmelb*–/– mutants at 12 dpf. The melanophores in the head and RPE were similar to the situation revealed in *pmela*–/– mutants. (K and K') *pmela*–/–;*pmelb*–/– mutants were detected with global golden body color, but light gray pigmented melanophores were detected in some areas like the top head at 60 dpf. (L and L') *pmela*–/–;*pmelb*–/– mutants were detected with golden plumage body color, no bars, but similar light color pattern with *pmela*–/– and *pmelb*–/– mutants in the dorsal fin at 90 dpf. (M) Wild-type fish with global black plumage and hyperpigmented vertical bars detected on the trunk and fins at 150 dpf. (N) *pmela*–/–;*pmelb*–/– mutants were detected with complete golden plumage at 150 dpf.

which were the fundamental reason for the formation of golden body color in tilapia.

Discussion

Pmela and *pmelb* Showed Similar Expression Patterns in Nile Tilapia

Pmel is a key gene involved in melanin biosynthesis and the development of body color in many fish species, such as carp (Wang et al. 2014; Zhang et al. 2017) and cichlids (Henning et al. 2013; Zhu et al. 2016; Liang et al. 2020). In those studies, the expression levels of *pmela* in hyperpigmented skin were always significantly higher than in hypopigmented skin. In the skin transcriptome of Malaysian red tilapia, *pmela* was found to be expressed significant higher in black skin than in red/pink skin (Zhu et al. 2016), suggesting that *pmel* might be involved in skin color differentiation between black and red tilapia. Additionally, this study suggested that *pmela* and *pmelb* were most highly expressed in eyes, indicating that the 2 genes might be involved in eye pigmentation and development. In zebrafish, *pmela* has been shown to be involved in eye pigmentation and anterior segment size maintenance in early juvenile stages, through loss of function studies (Lahola-Chomiak et al. 2019). In different developmental stages of wild-type Nile tilapia, *pmela* and *pmelb* were detected with similar expression patterns. They were both highly expressed in early developmental stages (from 6 to 12 dpf), which was in consistent with the several waves of melanophore proliferation

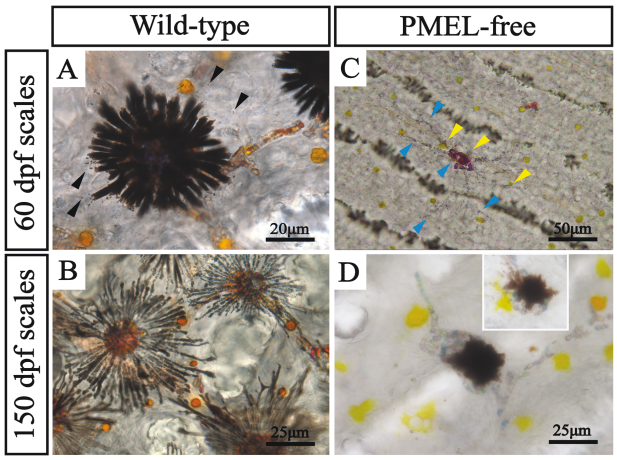

Figure 8. Effects of *pmela* and *pmelb* double mutation on pigment cell number, morphology, and location in scales of tilapia. In the wild type, most of the melanophores were young, with many dendrites and extracellular release of melanosomes at 60 dpf (A, black arrow). With the development, most of the melanophores became elder. The increased and further extended dendrites propelled the xanthophores far away from the main body of the melanophore at 150 dpf (B). In *pmela–/–;pmelb–/–* mutants, the main body and dendrites of the melanophore shrank, and accumulated a large amount of purple, blue and even red guanine due to the decreased ability of melanin synthesis. The xanthophores became closer to the melanophores at 60 dpf (C, yellow arrow). At 150 dpf, the main body, but not the dendrites, was filled with melanosome, due to the partially recovered melanin synthesis ability. Xanthophores were obviously enlarged with "airememes" in the mutants compared with those of the wild type (D).

identified in our previous studies of color patterning in Nile tilapia (Wang et al. 2021). However, no expression of *pmela* and *pmelb* was detected at 2–4 dpf, probably because these genes are downstream in the melanogenesis pathway, and follow the expression of NCCs-melanophores specification genes like *mitf* and *kita/kitlga*. Moderate expression of *pmela* and *pmelb* was also detected in fish at 30–90 dpf and the adult stage, suggesting that they are probably involved in melanin biosynthesis or melanophore survival at later stages. The *pmelb* was detected with some expression in dorsal fins in adult wild-type fish, which was in accordance with the results of our loss of function studies. The $pmela^{-/-}$ mutants were still observed with banding in dorsal fin at 60 dpf, whereas $pmelb^{-/-}$ mutants presented a more serious hypopigmentation of this fin. This was similar to the expression analysis in the cichlid, *Neolamprologus meeli*, in which higher *pmel* expression was detected in adult dorsal fin than in the ventral part of the anal fin or the caudal fin (Ahi et al. 2017).

Homozygous Mutation of *pmel* Genes Resulted in Golden Color in Tilapia

Using CRISPR/Cas9 gene editing, we successfully disrupted the expression of PMEL. Different levels of hypopigmentation were detected in the F0 mutants (Wang et al. 2021). As predicted, the homozygous mutants of *pmela*, *pmelb*, and *pmela;pmelb* all showed obvious hypopigmentation, while the overall performance and behavior of the mutants were not influenced. All 3 mutants had yellowish/golden body color, especially in the double mutants. The $pmela^{-/-};pmelb^{-/-}$ double mutants had completely golden bodies, without any black/gray patches or spots, which made them quite attractive (Figure 7N and Supplementary Figure S9). However, the golden fish had pigment patterning in fins. This was similar to studies in zebrafish, in which disruption of *csf1ra*, a xanthophore differentiation marker, led to different phenotypes in trunk and fins (Parichy and Turner 2003). Additionally, studies of pigment cells in *Danio* and other teleosts also suggested that color patterns in trunk and fins are probably controlled by different genes (Lewis et al. 2019; Patterson and Parichy 2019). In a recently published manuscript, the gene *pmel17* (*pmela*) was found to be closely linked with color traits in a naturally mutant yellow Mozambique tilapia population (Liu et al. 2021). It should be highlighted that *pmel* mutation on mice only alters the melanosome shapes, while has no influences on visible coat coloration (Hellström et al. 2011). Similarly, loss of function of *pmel* in chicken and quail resulted in milder hypopigmentation (Kerje et al. 2004; Watt et al. 2011; Ishishita et al. 2018). As a contrast, in *pmela* disrupted zebrafish (Lahola-Chomiak et al. 2019) and *pmel* disrupted tilapia, serious hypopigmentation was detected across the whole fish, as revealed by melanophore deficiency and insufficient melanin biosynthesis. These results suggested that *pmel* has a more critical role for pigmentation in fishes than in mammals and birds.

The Effects of PMEL Mutation on Pigment Cells Relative Abundance and Melanin Biosynthesis in Nile Tilapia

As mentioned above, loss of function of both *pmela* and *pmelb* in Nile tilapia led to a complete golden skin color without any black bars or patches, but with hypopigmented eyes, due to the increased numbers and sizes of xanthophores, and decreased numbers and sizes of melanophores, as well as hypopigmentation reflected by deficient in melanin biosynthesis (Figures 8 and 9A and B).

Some of the melanin-free melanophores were able to accumulate guanine, especially in early developmental stages (stages before 60 dpf). During the time period the pigmentary basis for the continued presence of banding in the fins of mutant fish were bands of guanine. We did not detect red erythrophores until at least 50 dpf in our previous studies (Wang et al. 2021), and the sizes and shapes were most similar to melanophores. The 60 dpf wild-type fish also showed many melanophores with different levels of black/gray melanin. Previous studies on zebrafish suggested that melanophores were still detected in *tyr* homozygous mutants, but they did not contain melanin pigment (Taylor et al. 2011). Our results are similar to those from zebrafish *tyr* mutants, but the tilapia PMEL-free mutants displayed milder defects compared to the zebrafish *tyr* mutants.

Melanophores size was also affected by mutation of *pmel*, as melanophores were smaller in the mutants, not only in the whole trunk and fins, but also in the scales (Figures 8D and 9B). This is likely to be a result of defects in forming a fibrillar structure within the melanosome upon which melanin is deposited (Watt et al. 2013; Christin et al. 2016), which finally led to the appearance of small melanophores with insufficient melanosome development.

At the same time, mutation of *pmel* genes caused increases in the numbers and sizes of xanthophores, which plays a decisive role in the complete golden phenotype. In wild-type fish, xanthophores are small and round in shape, whereas the neighboring melanophores are dendritic. In

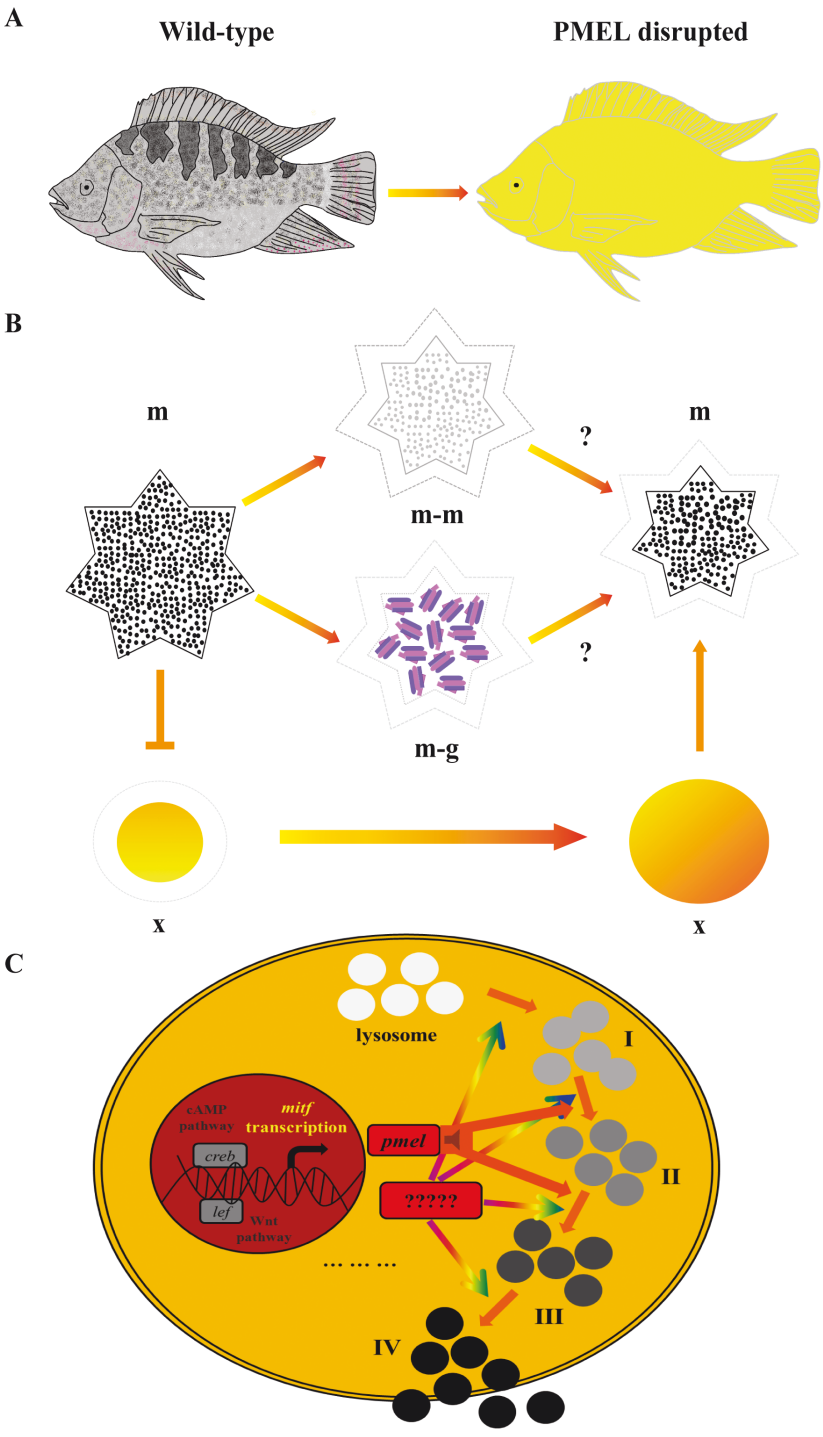

Figure 9. Proposed model of PMEL disruption in this study. (A) Disruption of *pmela* and *pmelb* resulted in complete golden plumage and hypopigmentation in eyes of tilapia. (B) Disruption of *pmela* and *pmelb* resulted in decreased and hypopigmented melanophores, and even guanine biosynthesis in not pigmented melanophores. Additionally, melanophores size was also heavily reduced in it. Disruption of *pmela* and *pmelb* also resulted in increased and larger sized xanthophores, which was another key reason for complete golden plumage. In wild-type fish, larger sized melanophores rejected the size-restricted xanthophores, whereas in PMEL-free mutants, the xanthophores with larger size than in wild-type fish pursuited the functionally restricted tiny melanophores. (C) Schematic view of melanin biosynthesis. *Mitf* as the key transcription factor for melanogenesis is responsible for cis-directing the *mitf*-axis downstream genes such as *pmel*. There are 4 phases of melanin, *pmel* was fundamental for both phases I–II and phases II–III melanin transition, thus hypopigmented melanophores were observed in PMEL disrupted tilapia. However, restoration of melanin biosynthesis was observed in PMEL disrupted tilapia, suggesting that additional collateral branches and some other key genes might be involved in melanin biosynthesis. The unknown gene was probably related to melanin biosynthesis from phase I to phase IV, and even lysosome biosynthesis. m, melanophores; m-m, melanophores with immature melanin; m-g, melanophores fulfilled with guanine; x, xanthophores.

pmela$^{-/-}$;*pmelb*$^{-/-}$ mutants, xanthophores were larger than in wild-type fish, whereas melanophores were detected with spot-like shapes, not only in the trunk surface and fins, but also in the scales (Figures 8C, D and 9B).

Mitf is a key transcription factor for melanin biosynthesis and is necessary for all the processes from the development of melanosomes to mature melanin release. Both *pmel* genes have promoter sequences that suggest they are regulated by *mitf*. Probably *pmel* was critical for melanosome transition from phase I to III, as we detected hypopigmented melanophores with light gray melanin in PMEL-disrupted fish. However, we detected slow restoration of melanin biosynthesis during development (Figure 9C), possibly because some melanin synthesis can occur in the absence of the fibrillar substrate provided by PMEL. Even though melanin could accumulate gradually over many weeks, the mutants did not produce a melanin-pigmented phenotype as the melanophores were small.

Pmela Was More Important Than *pmelb* in RPE Pigmentation and Eye Development

In this study, both *pmela* and *pmelb* were detected with the highest expression levels in the eyes of wild-type fish. They were further proved to be involved in eye pigmentation by our loss of function studies. Significant less global pigment was detected in the eyes of *pmel-a*$^{-/-}$ and *pmela*$^{-/-}$;*pmelb*$^{-/-}$ mutants. *Pmela* was further confirmed to be necessary for eye pigmentation (hypopigmentation of the RPE and iris) in early stages of eye development, which was in consistent with the results from human and zebrafish (Lahola-Chomiak et al. 2019). In a phylogenetic analysis across different fish species, *pmelb* was suggested to be responsible for adaptive phenotypes (specifically melanin-free in both eyes and the whole trunk, and eye degeneration) in extreme environments (Bian et al. 2021). In our studies, disruption of *pmela* resulted in RPE pigment loss. The *pmela*$^{-/-}$ and *pmela*$^{-/-}$;*pmelb*$^{-/-}$ mutants had a deep red RPE and also a hypopigmented iris, whereas the *pmelb*$^{-/-}$ mutants had an almost normal pigmented RPE, but a hypopigmented iris. The results indicate that both *pmela* and *pmelb* are critical for iris pigmentation, whereas *pmela* played a more important role than *pmelb* in RPE pigmentation and eye development in tilapia. Whether this is true in other teleosts species remains to be investigated.

Both *pmela* and *pmelb* Were Important for Body Color Formation in Nile Tilapia

Although many studies of gene expression suggested that *pmel* might function in body color differentiation (Henning et al. 2013; Zhu et al. 2016; Wang et al. 2014; Zhang et al. 2017; Liang et al. 2020), ours is the first detailed functional analysis of *pmela* and *pmelb* in teleosts. The effects of *pmel* mutations appear to vary among species (Kerje et al. 2004; Hellström et al. 2011). *Pmel* mutation has been confirmed to be the main cause of eye abnormal development including RPE pigment loss and anterior segment abnormal development in human beings and zebrafish (Lahola-Chomiak et al. 2019). The phenotypes of *pmela* mutants in tilapia, hypopigmentation of trunk surface and RPE, were similar to those revealed in larvae zebrafish.

Body color is an important economic trait. In aquaculture, the fish with pleasant body color is always preferred by consumers. For example, the koi carp and golden fish have been raised as pet fish all over the world, due to their attractive body color or amazing specific color patterns. In tilapia, the red tilapia is also preferred by consumers globally because of the lack of black pigmentation in the trunk and peritoneum (Huang et al. 1988; McAndrew et al. 1988). The establishment of a golden tilapia (*pmela*$^{-/-}$;*pmelb*$^{-/-}$ mutants) would be of great significance to the tilapia aquaculture industry, and might also be of interest in the pet fish market.

Supplementary Material

Supplementary data are available at *Journal of Heredity* online.

Funding

This work was supported by grants 31872556, 31861123001 and 31630082 from the National Natural Science Foundation of China; grants CYS17080 from the Chongqing Municipal Education Commission.

Conflict of Interest

The authors declare that they have no known competing financial interests or personal relationships that could have appeared to influence the work reported in this paper.

Data Availability

All data are available in the text and Supplementary Materials.

References

Ahi EP, Sefc KM. 2017. A gene expression study of dorso-ventrally restricted pigment pattern in adult fins of *Neolamprologus meeli*, an African cichlid species. *PeerJ*. 5:e2843.

Bian C, Li R, Wen Z, Ge W, Shi Q. 2021. Phylogenetic analysis of core melanin synthesis genes provides novel insights into the molecular basis of albinism in fish. *Front Genet*. 12:707228.

Bilandžija H, Abraham L, Ma L, Renner KJ, Jeffery WR. 2018. Behavioural changes controlled by catecholaminergic systems explain recurrent loss of pigmentation in cavefish. *Proc Biol Sci*. 285(1878): 20180243.

Bilandžija H, Ma L, Parkhurst A, Jeffery WR. 2013. A potential benefit of albinism in Astyanax cavefish: downregulation of the oca2 gene increases tyrosine and catecholamine levels as an alternative to melanin synthesis. *PLoS One*. 8:e80823.

Braasch I, Brunet F, Volff JN, Schartl M. 2009. Pigmentation pathway evolution after whole-genome duplication in fish. *Genome Biol Evol*. 1:479–493.

Brawand D, Wagner CE, Li YI, Malinsky M, Keller I, Fan S, Simakov O, Ng AY, Lim ZW, Bezault E, et al. 2014. The genomic substrate for adaptive radiation in African cichlid fish. *Nature*. 513:375–381.

Christin B, Leila R, Guillaume VN. 2016. PMEL amyloid fibril formation: the bright steps of pigmentation. *Int J Mol Sci*. 17(9): 1438.

Espinasa L, Robinson J, Espinasa M. 2018. Mc1r gene in *Astroblepus pholeter* and *Astyanax mexicanus*: convergent regressive evolution of pigmentation across cavefish species. *Dev Biol*. 441:305–310.

Frolov AS, Pika IS, Eroshkin AM. 1997. ProMSED: protein multiple sequence editor for Windows 3.11/95. *Comput Appl Biosci*. 13:243–248.

Gross JB, Wilkens H. 2013. Albinism in phylogenetically and geographically distinct populations of Astyanax cavefish arises through the same loss-of-function Oca2 allele. *Heredity (Edinb)*. 111:122–130.

Gutknecht M, Geiger J, Joas S, Dörfel D, Salih HR, Müller MR, Grünebach F, Rittig SM. 2015. The transcription factor MITF is a critical regulator of GPNMB expression in dendritic cells. *Cell Commun Signal*. 13:19.

Hattori RS, Yoshinaga TT, Butzge AJ, Hattori-Ihara S, Tsukamoto RY, Takahashi NS, Tabata YA. 2020. Generation of a white-albino phenotype from cobalt blue and yellow-albino rainbow trout (*Oncorhynchus mykiss*): inheritance pattern and chromatophores analysis. *PLoS One*. 15:e0214034.

Hellström AR, Watt B, Fard SS, Tenza D, Mannström P, Narfström K, Ekesten B, Ito S, Wakamatsu K, Larsson J, et al. 2011. Inactivation of Pmel alters melanosome shape but has only a subtle effect on visible pigmentation. *PLoS Genet*. 7:e1002285.

Hendrick LA, Carter GA, Hilbrands EH, Heubel BP, Schilling TF, Le Pabic P. 2019. Bar, stripe and spot development in sand-dwelling cichlids from Lake Malawi. *Evodevo*. 10:18.

Henning F, Jones JC, Franchini P, Meyer A. 2013. Transcriptomics of morphological color change in polychromatic Midas cichlids. *BMC Genomics*. 14:171.

Hoekstra HE. 2006. Genetics, development and evolution of adaptive pigmentation in vertebrates. *Heredity (Edinb)*. 97:222–234.

Hofreiter M, Schöneberg T. 2010. The genetic and evolutionary basis of colour variation in vertebrates. *Cell Mol Life Sci*. 67:2591–2603.

Hou L, Pavan WJ. 2008. Transcriptional and signaling regulation in neural crest stem cell-derived melanocyte development: do all roads lead to Mitf? *Cell Res*. 18:1163–1176.

Huang CM, Chang SL, Cheng HJ, Liao IC. 1988. Single gene inheritance of red body coloration in Taiwanese red tilapia. *Aquaculture*. 74: 227–232.

Hubbard JK, Uy JA, Hauber ME, Hoekstra HE, Safran RJ. 2010. Vertebrate pigmentation: from underlying genes to adaptive function. *Trends Genet*. 26:231–239.

Ishishita S, Takahashi M, Yamaguchi K, Kinoshita K, Nakano M, Nunome M, Kitahara S, Tatsumoto S, Go Y, Shigenobu S, et al. 2018. Nonsense mutation in PMEL is associated with yellowish plumage colour phenotype in Japanese quail. *Sci Rep*. 8:16732.

Ito S, Wakamatsu K. 2011. Human hair melanins: what we have learned and have not learned from mouse coat color pigmentation. *Pigment Cell Melanoma Res*. 24:63–74.

Kerje S, Sharma P, Gunnarsson U, Kim H, Bagchi S, Fredriksson R, Schütz K, Jensen P, von Heijne G, Okimoto R, et al. 2004. The Dominant white, Dun and Smoky color variants in chicken are associated with insertion/deletion polymorphisms in the PMEL17 gene. *Genetics*. 168:1507–1518.

Klaassen H, Wang Y, Adamski K, Rohner N, Kowalko JE. 2018. CRISPR mutagenesis confirms the role of oca2 in melanin pigmentation in *Astyanax mexicanus*. *Dev Biol*. 441:313–318.

Kratochwil CF, Liang Y, Gerwin J, Woltering JM, Urban S, Henning F, Machado-Schiaffino G, Hulsey CD, Meyer A. 2018. Agouti-related peptide 2 facilitates convergent evolution of stripe patterns across cichlid fish radiations. *Science*. 362:457–460.

Kwon BS, Kim KK, Halaban R, Pickard RT. 1994. Characterization of mouse Pmel 17 gene and silver locus. *Pigment Cell Res*. 7:394–397.

Lahola-Chomiak AA, Footz T, Nguyen-Phuoc K, Neil GJ, Fan B, Allen KF, Greenfield DS, Parrish RK, Linkroum K, Pasquale LR, et al. 2019. Non-synonymous variants in premelanosome protein (PMEL) cause ocular pigment dispersion and pigmentary glaucoma. *Hum Mol Genet*. 28:1298–1311.

Lewis VM, Saunders LM, Larson TA, Bain EJ, Sturiale SL, Gur D, Chowdhury S, Flynn JD, Allen MC, Deheyn DD, et al. 2019. Fate plasticity and reprogramming in genetically distinct populations of *Danio leucophores*. *Proc Natl Acad Sci USA*. 116:11806–11811.

Liang Y, Gerwin J, Meyer A, Kratochwil CF. 2020. Developmental and cellular basis of vertical bar color patterns in the East African cichlid fish *Haplochromis latifasciatus*. *Front Cell Dev Biol*. 8:62.

Liu F, Sun F, Kuang GQ, Wang L, Yue GH. 2021. Identification of *Pmel17* for golden skin color using linkage mapping in *Mozambique tilapia*. *Aquaculture*. 548:737703.

Loftus SK, Antonellis A, Matera I, Renaud G, Baxter LL, Reid D, Wolfsberg TG, Chen Y, Wang C, Prasad MK, et al.; NISC Comparative Sequencing Program. 2009. Gpnmb is a melanoblast-expressed, MITF-dependent gene. *Pigment Cell Melanoma Res*. 22:99–110.

McAndrew BJ, Roubal FR, Roberts RJ, Bullock AM. 1988. Mcewen I. M. The genetics and histology of red, blond and associated colour variants in *Oreochromis niloticus*. *Genetica*. 76(2): 127–137.

O'Quin CT, Drilea AC, Conte MA, Kocher TD. 2013. Mapping of pigmentation QTL on an anchored genome assembly of the cichlid fish, Metriaclima zebra. *BMC Genomics*. 14:287.

Parichy DM, Turner JM. 2003. Temporal and cellular requirements for Fms signaling during zebrafish adult pigment pattern development. *Development*. 130:817–833.

Patterson LB, Parichy DM. 2019. Zebrafish pigment pattern formation: insights into the development and evolution of adult form. *Annu Rev Genet*. 53:505–530.

Roberts RB, Moore EC, Kocher TD. 2017. An allelic series at pax7a is associated with colour polymorphism diversity in Lake Malawi cichlid fish. *Mol Ecol*. 26:2625–2639.

Santos ME, Braasch I, Boileau N, Meyer BS, Sauteur L, Böhne A, Belting HG, Affolter M, Salzburger W. 2014. The evolution of cichlid fish egg-spots is linked with a cis-regulatory change. *Nat Commun*. 5:5149.

Schneider CA, Rasband WS, Eliceiri KW. 2012. NIH Image to ImageJ: 25 years of image analysis. *Nat Methods*. 9:671–675.

Stahl BA, Gross JB. 2015. Alterations in Mc1r gene expression are associated with regressive pigmentation in Astyanax cavefish. *Dev Genes Evol*. 225:367–375.

Sun YL, Jiang DN, Zeng S, Hu CJ, Ye K, Yang C, Wang D. 2014. Screening and characterization of sex-linked DNA markers and marker-assisted selection in the Nile tilapia (*Oreochromis niloticus*). *Aquaculture*. 433: 19–27.

Tamura K, Stecher G, Peterson D, Filipski A, Kumar S. 2013. MEGA6: Molecular Evolutionary Genetics Analysis version 6.0. *Mol Biol Evol*. 30:2725–2729.

Taylor KL, Lister JA, Zeng Z, Ishizaki H, Anderson C, Kelsh RN, Jackson IJ, Patton EE. 2011. Differentiated melanocyte cell division occurs in vivo and is promoted by mutations in Mitf. *Development*. 138:3579–3589.

Wang C, Lu B, Li T, Liang G, Xu M, Liu X, Tao W, Zhou L, Kocher TD, Wang D. 2021. Nile tilapia: a model for studying teleost color patterns. *J Hered*. 112:469–484.

Wang K, Shen Y, Yang Y, Gan X, Liu G, Hu K, Li Y, Gao Z, Zhu L, Yan G, et al. 2019. Morphology and genome of a snailfish from the Mariana Trench provide insights into deep-sea adaptation. *Nat Ecol Evol*. 3:823–833.

Wang C, Wachholtz M, Wang J, Liao X, Lu G. 2014. Analysis of the skin transcriptome in two oujiang color varieties of common carp. *PLoS One*. 9:e90074.

Watanabe M, Kondo S. 2015. Is pigment patterning in fish skin determined by the Turing mechanism? *Trends Genet*. 31:88–96.

Watt B, Tenza D, Lemmon MA, Kerje S, Raposo G, Andersson L, Marks MS. 2011. Mutations in or near the transmembrane domain alter PMEL amyloid formation from functional to pathogenic. *PLoS Genet*. 7:e1002286.

Watt B, van Niel G, Raposo G, Marks MS. 2013. PMEL: a pigment cell-specific model for functional amyloid formation. *Pigment Cell Melanoma Res*. 26:300–315.

Yamaguchi Y, Hearing VJ. 2009. Physiological factors that regulate skin pigmentation. *Biofactors*. 35:193–199.

Yuan X, Meng D, Cao P, Sun L, Pang Y, Li Y, Wang X, Luo Z, Zhang L, Liu G. 2019. Identification of pathogenic genes and transcription factors in vitiligo. *Dermatol Ther*. 32:e13025.

Zhang Y, Liu J, Peng L, Ren L, Zhang H, Zou L, Liu W, Xiao Y. 2017. Comparative transcriptome analysis of molecular mechanism underlying gray-to-red body color formation in red crucian carp (*Carassius auratus*, *red var.*). *Fish Physiol Biochem*. 43:1387–1398.

Zhao Q, Zhang R, Xiao Y, Niu Y, Shao F, Li Y, Peng Z. 2019. Comparative transcriptome profiling of the loaches *Triplophysa bleekeri* and *Triplophysa rosa* reveals potential mechanisms of eye degeneration. *Front Genet*. 10:1334.

Zhu W, Wang L, Dong Z, Chen X, Song F, Liu N, Yang H, Fu J. 2016. Comparative transcriptome analysis identifies candidate genes related to skin color differentiation in red tilapia. *Sci Rep*. 6:31347.